UCRL - 74743
PREPRINT
Conf-730301--7

LAWRENCE LIVERMORE LABORATORY
University of California/Livermore, California

Systematic Properties of the Giant Resonance: Current Status

R. L. Bramblett
S. C. Fultz
B. L. Berman

May 4, 1973

This paper was prepared for submittal to the Proceedings of the International Conference on Photonuclear Reactions and Applications.

SYSTEMATIC PROPERTIES OF THE GIANT RESONANCE: CURRENT STATUS†

R. L. Bramblett
Gulf Radiation Technology
P. O. Box 81608, San Diego, California 92138

S. C. Fultz and B. L. Berman
Lawrence Livermore Laboratory
P. O. Box 808, Livermore, California 94550

PREFACE

This paper was originally scheduled to be presented by Stanley C. Fultz, who for sixteen years was the leader of photonuclear research done at Lawrence Livermore Laboratory. Stan Fultz died, following a brief illness, on June 18, 1972. A large portion of the photonuclear work reported here was done by Stan and his colleagues. He pioneered the Livermore work on the use of positron annihilation in flight for the systematic measurement of cross sections over the giant resonance, resulting in measurements for over 50 nuclei throughout the periodic table. He was personally responsible for the conception, design, and completion of the new 100 MeV Livermore Electron Positron Linear Accelerator, which is now producing the high quality photonuclear and neutron physics results that he envisioned. The coauthors of this paper were privileged to work with Dr. Fultz during his years at Livermore.

INTRODUCTION

The purpose of this paper is to summarize, from the viewpoint of an experimentalist, the outstanding systematic properties of the giant resonance for photonuclear reactions, as observed using real photons from about 8 to 35 MeV. In the last ten years the quality and quantity of photonuclear data in this energy region has improved remarkably, principally because of the emergence of the positron annihilation technique as pioneered by Fultz and his collaborators at Livermore, and Tzara, Bergere and others at Saclay. Other techniques for producing nearly monoenergetic photons have yielded important results, but not results in the quantity and over the range of nuclei that allow systematics to be evaluated.

ANNIHILATION PHOTON TECHNIQUE

An earlier experimental arrangement for positron annihilation-in-flight experiments at Livermore is shown in Figure 1. A figure of the new setup is given in Paper 2D16S of this Conference. Positrons, which are produced by electron bremsstrahlung and pair production in a W or Ta converter between sections of the Linac, are energy analyzed and directed onto a low-Z target where some annihilate with electrons of the target. Positrons that penetrate the annihilation target are bent away from the beam line with a magnet. The annihilation photons emitted in the direction of positron velocity are used to produce photonuclear reactions. At this angle (0°), the annihilation photon energy equals the positron energy plus 0.76 MeV. At Livermore, paraffin-moderated BF_3 proportional counters are used to detect neutrons, whereas at Saclay the neutron detector is a large Gd-loaded liquid scintillator. In either case, the multiplicity of neutrons produced per reaction can be determined so that (γ,n), $(\gamma,2n)$ and $(\gamma,3n)$ cross sections can be measured. For nuclei with A greater than 60, the sum of these cross sections is essentially the photon absorption cross section.

Another experimental measurement must be made using electrons incident on the annihilation target to correct for the positron bremsstrahlung accompanying the annihilation radiation. The correction is illustrated in Figure 2, which shows the photoneutron yields produced from Au when positrons or electrons are incident on the annihilation target. The subtraction of the electron data from positron data to obtain the signal produced by annihilation photons becomes a serious limitation to accuracy by 10 or 15 MeV above the giant resonance, because of the large statistical and normalization errors introduced.

†Work performed under the auspices of the U. S. Atomic Energy Commission.

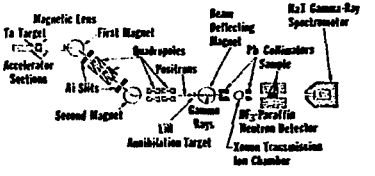

Figure 1. Apparatus for the measurement of photonuclear cross sections using photons from positron annihilation in flight.

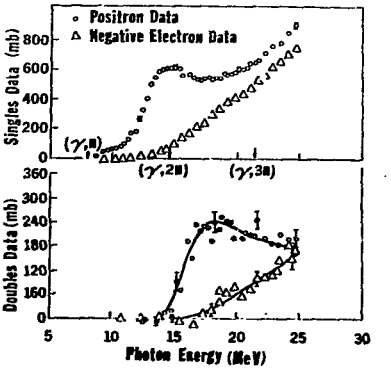

Figure 2. Photoneutron yields from positron and electron radiations.

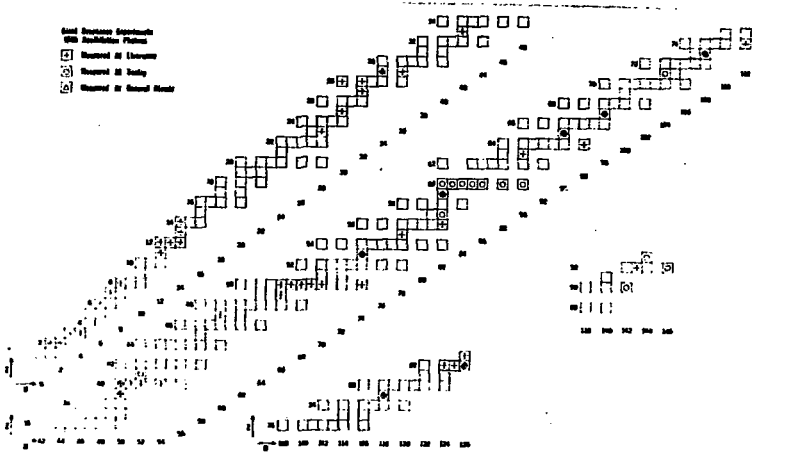

Figure 3. Nuclei for which cross sections have been measured using positron annihilation in flight.

NUCLEI STUDIED

At the present time, photonuclear cross sections have been measured using the annihilation-photon technique for approximately 68 nuclei, 45 of which are in the mass region above 50, where it is possible to consider systematic characteristics. A map of the nuclei studied is shown in Figure 3. B. L. Berman has compiled at atlas[1] of these cross sections, which is available from him upon request.

THE HYDRODYNAMIC MODEL

To be able to discuss the photonuclear characteristics over a broad range of nuclei we will use the two-fluid model of Goldhaber and Teller,[2] Steinwedel and Jensen,[3] and Danos.[4] Other papers in this conference will surely discuss the refinements and inadequacies of this model. According to the model, the photon absorption cross section for spheroidal nuclei may consist of one or two Lorentz curves.

$$\sigma(E) = \sum_{i=1}^{2} \frac{\sigma_i}{1 + \left(E^2 - E_i^2\right)^2 / E^2 \Gamma_i^2} \qquad (1)$$

$$\int \sigma(E)dE = \sum_{i=1}^{2} \frac{\pi}{2} \sigma_i \Gamma_i \quad . \qquad (2)$$

The model also predicts the energies of the giant resonance:

$$E_i = \left\{ 8 \frac{\hbar^2 c^2}{R_o^2} \frac{K}{Mc^2} \frac{NZ}{A^{8/3}} (k_i R)^2 - \frac{\Gamma_i^2}{4} \right\}^{\frac{1}{2}} . \qquad (3)$$

Here, R_o is the nuclear radius parameter ($R = R_o A^{1/3}$), K is the nuclear symmetry energy, and $k_i R$ are eigenvalues characteristic of deformation of the spheroid. Insofar as this model is concerned, the parameters are K, R_o, Γ_i, and the intrinsic quadrupole moment, which determines $k_i R$. The model makes no statement about the magnitude or origin of the widths, Γ_i, except that they are damping terms, analogous to viscosity.

For spherical nuclei, $k_i R = 2.082$, so that

$$E = \left\{ 1455 \frac{K}{R_o^2} \frac{NZ}{A^{8/3}} - \frac{\Gamma^2}{4} \right\}^{\frac{1}{2}} . \qquad (4)$$

Note that no effective mass corresponding to the existence of exchange forces has been introduced in the formula for the giant-resonance energy. Since R_o is reasonably well determined from electron scattering experiments, any effective mass correction must be buried in the symmetry energy parameter, K. As will be seen, the photonuclear data show that K/R_o^2 is a slowly varying function of A, with a value of K consistent with that used in semi-empirical mass formulae.

SELECTED RESULTS

An example of recent measurements which show systematic behavior of the giant resonance is the Nd series of isotopes measured at Saclay by Carlos et al.,[5] shown in Figure 4. The data have been fitted with Lorentz curves (two components in the case of ^{150}Nd). The peak energies decrease slightly with increasing neutron number, as expected from the model. As is the case for deformed nuclei, the quadrupole moment of ^{150}Nd can be determined from the energies of its two-component giant resonance. Lorentz curves fit the measured cross sections very well, with some small deviations on the low side of the giant resonance.

Another series, measured at Livermore by Berman et al.,[6] is for the Zr isotopes. The results for the photon absorption cross section of ^{90}Zr are shown in Figure 5. In this case, there is obvious structure on the high-energy side of the giant resonance that agrees in energy with predictions by Akyuz and Fallieros[7] of a $T = T_z + 1$ giant resonance. That the amplitude of this $T = T_z + 1$ component is less than the theoretical prediction is expected since neutron emission is isospin forbidden. There is a corresponding peak in the proton-emission channel, as seen by Dushkov et al.[8] It is likely that the structure seen in the Livermore experiment is a result of isospin mixing rather than decay through the (γ,pn) channel, since the energy above the (γ,pn) threshold is small. Several other Zr isotopes showed similar structure, with the same possible explanation. The $T = T_z + 1$ giant resonance is difficult to observe for nuclei very much heavier than mass 100, because

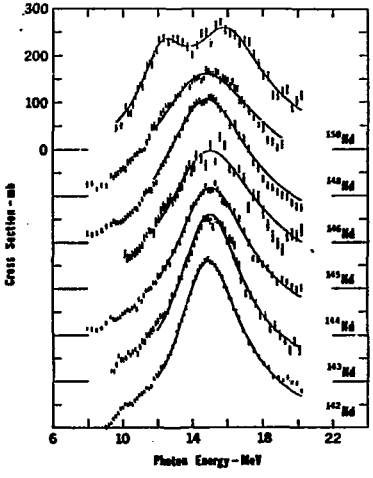

Figure 4. The photon absorption cross sections of the Nd isotopes. Smooth curves are Lorentz-curve fits to the data.

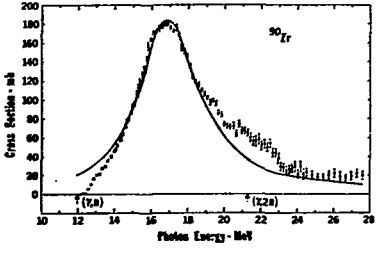

Figure 5. The photon absorption cross section of ^{90}Zr. The excess yield above the Lorentz curve is attributed to the $T = T_z + 1$ giant resonance.

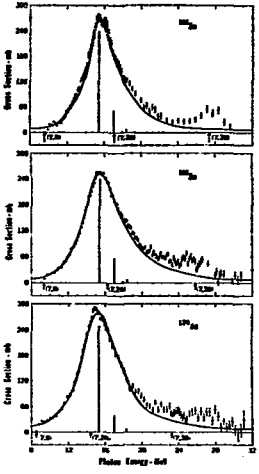

Figure 6. The photon absorption cross sections of the Sn isotopes.

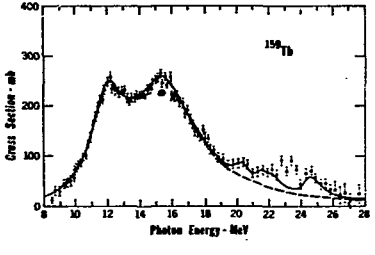

Figure 7. The total photon absorption cross section of ^{159}Tb. The solid curve is a result of calculation using the dynamic collective theory including the E2 giant resonance.

the $T = T_z + 1$ strength decreases rapidly with A. At lower A, the cross sections have other structure that makes the assignment difficult.

The Sn isotopes have been measured by Fultz et al.,[9] with results for three isotopes shown in Figure 6. Structure which may be the $T = T_z + 1$ resonance is seen above the main resonance. Calculations by Arenhovel and Greiner[10] using the dynamic collective model for electric dipole transitions do not include the structure. However, the structure might also be E2 photon absorption, as described by Ligensa and Greiner.[11]

Another example, ^{159}Tb, measured some years ago by Bramblett et al.[12] is shown in Figure 7. This giant resonance shows splitting due to the deformation of ^{159}Tb, and also shows a broad bump which has been interpreted as the quadrupole giant resonance by Ligensa and Grainer.[11]

AREA RATIOS FOR DEFORMED NUCLEI

One of the successes of the elementary hydrodynamic model was the prediction[13,14] of double-humped giant resonances for deformed nuclei. The lower-energy component is predicted to have one half the amplitude of the higher component. The experimental results confirm this area ratio only for the most deformed of nuclei, as shown in Figure 8. It appears that the area ratio is directly correlated with the quadrupole moment. The dynamic collective model has been shown[11,14] to give good agreement with the experimentally observed area ratios for ^{165}Ho and ^{159}Tb with some adjustment of parameters; however, even this more refined model appears to be in disagreement with measurements of area ratios on polarized ^{165}Ho.

The measurement of the photon absorption cross section of polarized ^{165}Ho, made by Kelly et al.,[15] was both a lucid confirmation and a severe test of the hydrodynamic model. Figure 9 shows the cross sections as a function of energy obtained with the holmium target polarized parallel and perpendicular to the photon beam. With parallel polarization, the high-energy component of the giant resonance increases in amplitude because it corresponds to oscillation of the protons against neutrons in the directions transverse to the nuclear symmetry axis. Conversely, the low-energy component is increased when the target is polarized perpendicular to the photon beam. In fact, the observed change in amplitudes was only (75 ± 13)% of the change predicted by both the elementary hydrodynamic model and the dynamic collective model. The shape of the intrinsic cross sections, which Kelly et al. obtained for oscillations parallel and perpendicular to the nuclear symmetry axis, is clearly not Lorentzian, and appears to indicate coupling between the two modes.

DECAY MODES OF THE GIANT RESONANCE

There is interesting physics involved in the decay mode of the giant resonance, once it is excited by photons. First of all, the decay mode is predominantly statistical, as shown by the branching between the (γ,n), $(\gamma,2n)$, and $(\gamma,3n)$ cross sections. The ratio of $(\gamma,2n)$ to the total cross section can be calculated on a density-of-states argument, with the result:

$$\frac{\sigma(\gamma,2n)}{\sigma(\gamma,\text{total})} = \frac{\int_0^{E_\gamma - E_{thr}(\gamma,2n)} \rho(U) E_n \, dE_n}{\int_0^{E_\gamma - E_{thr}(\gamma,n) - \Delta} \rho(U) E_n \, dE_n} . \qquad (5)$$

Here, ρ is the level density in the target-minus-one-neutron nucleus and U is the excitation energy, corrected for pairing and shell effects:

$$U = E_\gamma - E_{thr}(\gamma,n) - E_n - \Delta . \qquad (6)$$

The theory predicts, and experiments confirm, that the (γ,n) cross section goes essentially to zero by 2 to 3 MeV above the $(\gamma,2n)$ threshold. Likewise, the $(\gamma,2n)$ yield disappears shortly above the $(\gamma,3n)$ threshold.

These experimental observations are illustrated in Figure 10, which shows the (γ,n), $(\gamma,2n)$, and $(\gamma,3n)$ cross sections of ^{165}Ho as reported by Berman et al.[15]

There is some experimental evidence, particularly by Axel and coworkers[16,17] and Bertozzi et al.,[18] that has been interpreted to indicate that as much as 25%, but more typically 10 to 15%, of the giant-resonance decays are nonstatistical. The data involved is the excess of high-

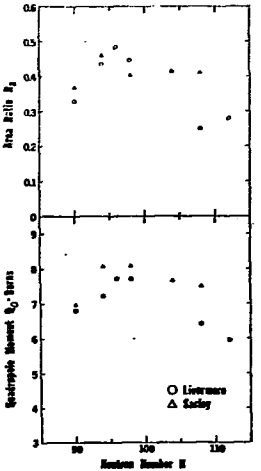

Figure 8. Area ratio of Lorentz-curve fits to photon absorption cross sections of deformed nuclei. The quadrupole moment is shown for comparison.

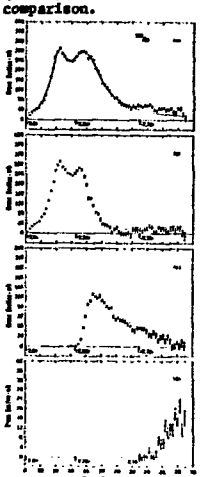

Figure 10. The photoneutron cross sections of ^{165}Ho. (a) total, (b) (γ,n), (c) (γ,2n), (d) (γ,3n).

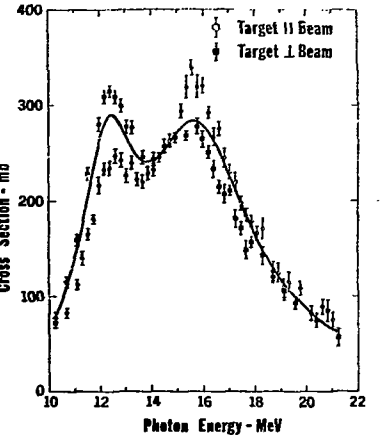

Figure 9. The photon absorption cross section of polarized ^{165}Ho. The curve is the Lorentz-curve fit to the unpolarized data.

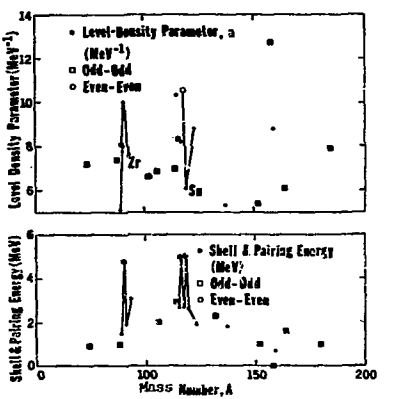

Figure 11. Level-density parameters obtained from the ratio of the (γ,2n) to the total photoneutron cross section.

energy neutrons over that predicted by statistical theories. However, the results of these experiments are sensitive to the shape assumed for the (inverse) cross section for the neutron interaction with the residual nucleus. The Livermore results on (γ,n) cross sections above the $(\gamma,2n)$ thresholds do not rule out a nonzero component of the order of 10%; the Saclay results seem to indicate a bit more nonstatistical decay.

Figure 11 shows the level-density parameter obtained for several nuclei from the analysis of the energy-dependent ratio of the $(\gamma,2n)$ cross section to the total neutron cross section. There is no particular trend in these values, but they do lie in the range expected from other types of determinations, such as inelastic scattering of neutrons. The correction to residual excitation energy for suppression of the ground state, which also is obtained from the ratio of cross sections, shows a marked even-even effect, as expected. However, there appears to be no marked difference in the ground state suppression of odd-A and odd-odd nuclei, although one would expect that odd-A suppression should be the larger.

At this point, it would be appropriate to summarize the contribution of (γ,p) reactions to the total photon cross section. However, (γ,p) cross sections are small and difficult to measure for nuclei with A > 60, so that too little data is available to summarize.

GIANT-RESONANCE WIDTHS

The rather large observed widths for the giant resonance have been a thorn in the side of both theorists and experimentalists. The latter have struggled for years to find structure that would give insight to the nuclear processes involved, only to find broad bumps and small undulations. The former have applied elegant theories to explain reported structure that melted away under heated scrutiny. Warm controversy still surrounds the subject. (See Berman et al., paper BE11 of this Conference.)

It does appear that the theories which originally were applied to explain nonexistent structure are being successfully applied to explain the giant-resonance widths. For nuclei that are very stiff toward surface vibrations, such as ^{90}Zr, ^{116}Sn, ^{142}Nd, and ^{208}Pb, the experimental width of the giant resonance is as small as about 4 MeV. This is illustrated in Figure 12, which shows the widths measured for spherical nuclei. As the stiffness toward surface vibrations decreases, the coupling to the dipole mode increases and the width increases. This is seen dramatically in the several experiments on the isotopes of a single element.

Assuming that the intrinsic width of individual dipole transitions has the form [19]

$$\Gamma = \Gamma_0 (E_\gamma / E_0)^\delta,$$

comparisons of calculations using the dynamic collective model with experiments on both deformed and spherical nuclei indicate that the parameters are

$$\Gamma_0 = 2.5,\ E_0 = 12.3,\ \delta = 2.4.$$

At E_γ= 15 MeV, the intrinsic width would then be 4.0 MeV, which is about the minimum width observed experimentally for spherical nuclei. Arenhovel and Greiner[10] used $\Gamma_0 = 2.5$ and $\delta = 1.6$, which give a width of 3.5 MeV at 15 MeV.

The widths of the two resonance components for deformed and vibrational nuclei are shown in Figure 13. The higher-energy resonance is always wider, as one would expect from the energy dependence of the individual components. A direct comparison of the two widths in the region of statically deformed nuclei would imply an energy exponent of 2.5 or less, depending on the extent of spreading of the dipole strength in the upper-energy resonance. It is interesting that this value agrees with the value obtained by comparison of dynamic-collective-model calculations with experiment.

GIANT-RESONANCE ENERGIES

The positions of the giant-resonance energies apparently are not influenced very much by coupling to surface vibrations, since the elementary hydrodynamic model gives a quite good description of the energies with only one slowly varying parameter, K, the nuclear symmetry energy.

Note that, according to Eq. (4), the giant-resonance energy depends upon the ratio K/R_0^2. For the present parameterization we assume that $R_0 = 1.20$ F.

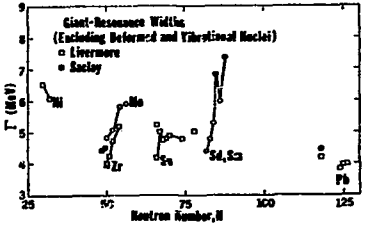

Figure 12. Giant-resonance widths for spherical nuclei.

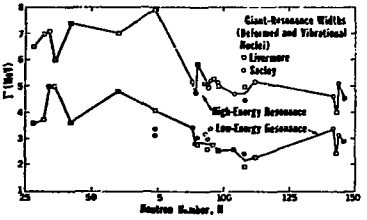

Figure 13. Widths of the two components of Lorentz-curve fits to the giant resonance of deformed and vibrational nuclei.

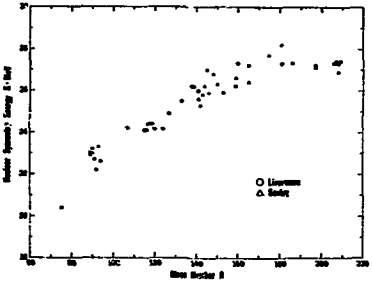

Figure 14. Nuclear symmetry energy obtained from energies of the giant resonance.

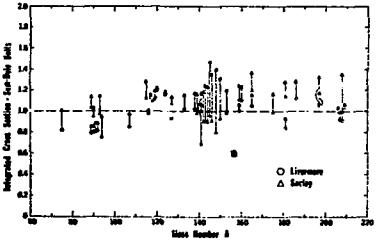

Figure 15. Integrated photonuclear cross sections for nuclei measured with the annihilation-in-flight technique. The arrow tips indicate the cross sections of the Lorentz-curve fits to the data.

The same value of K applies to both spherical and deformed nuclei. The symmetry energy is shown as a function of number in Figure 14. To an accuracy of about 5%, $K = 126\ (N/A)^3$, where N is the neutron number. For further discussion about K, see paper 5B15S of this Conference by B. L. Berman.

The spread in the experimentally determined values of K at a given value of A can be seen to be about ±1/3 MeV from the average. Consequently, using K determined from systematics and the intrinsic quadrupole moment, the giant-resonance energies of any nucleus with A > 80 can be predicted with an accuracy of about 100 keV, which is probably better than could be obtained in a single experiment. The value assumed for Γ is not very important; one MeV change in Γ leads to about 70 keV change in giant-resonance energy. Γ could be adequately estimated from systematics.

SUM RULES

With a few small-amplitude exceptions, the giant-resonance cross sections up to 35 MeV and for A > 60 can be described well by one or two Lorentz-shaped components. However, the data do not extend below the (γ,n) threshold or higher than about 35 MeV. Consequently, when comparing the sum

$$\sigma[(\gamma,n) + (\gamma,2n) + (\gamma,3n) + (\gamma,pn)]$$

to even model-independent sum rules, it is desirable to add to the data corrections for the unmeasured cross section. If the cross-section shape is indeed Lorentzian, the straightforward way to make the correction for the TRK sum rule is to compute the area under the Lorentz curves;

$$\frac{\pi}{2}\sum_{i=1}^{2}\sigma_i\Gamma_i \quad .$$

There are cases where this procedure is questionable, particularly when there are $T = T_z + 1$ bumps. However, we do want to exclude quadrupole bumps when comparing with the dipole sum rule. Hence, in Figure 15 are presented both the integral of the uncorrected data and the area of the fitted curves. The areas are divided by the TRK sum rule with no exchange correction: 60NZ/A MeV-mb. It appears that there are some discrepancies between the Livermore and Saclay values. This is principally associated with a larger extrapolation for the unmeasured cross section for the Saclay data.

Because of the rather large uncertainty in the unmeasured component of the photon absorption cross section near and below the (γ,n) threshold, the 1/E and $1/E^2$ weighted sum rules are even more difficult than the TRK sum rule to evaluate from photoneutron data. Total absorption experiments do offer the possibility of more meaningful comparison with higher-order sum rules.

The integrated cross sections, even including the unmeasured portion of the Lorentz curves, exceed the TRK sum rule, uncorrected for exchange forces, by an average of about 10%. If the exchange contribution to the cross section is more than 10%, the cross section must exceed the Lorentzian curve in the region above 35 MeV. Typically, an additional constant cross section of only 10 mb from 35 MeV to 135 MeV would add 50% to the cross section, but this will surely be one of the topics covered by Dr. Ziegler in the following paper.

REFERENCES

1 B. L. Berman, UCRL-74622 (unpublished).

2 M. Goldhaber and E. Teller, Phys. Rev. 74, 1046 (1948).

3 H. Steinwedel and J. H. D. Jensen, Z. Naturforsch. 5a, 413 (1950).

4 M. Danos, Nucl. Phys. 5, 23 (1958).

5 P. Carlos, H. Beil, R. Bergère, A. Lepretre, and A. Veyssière, Nucl. Phys. A172, 437 (1971).

6 B. L. Berman, J. T. Caldwell, R. R. Harvey, M. A. Kelly, R. L. Bramblett, and S. C. Fultz, Phys. Rev. 162, 1098 (1967).

7 R. O. Akyüz and S. Fallieros, Phys. Rev. Letters 27, 1016 (1971).

8 I. I. Dushkov, B. S. Ishkhanov, I. M. Kapitonov, E. A. Yur'ev and V. G. Shevchenko, Phys. Letters 10, 310 (1964).

9 S. C. Fultz, B. L. Berman, J. T. Caldwell, R. L. Bramblett, and R. R. Harvey, Phys. Rev. 186, 1255 (1969).

10 H. Arenhovel and W. Greiner, Progress in Nuclear Physics, 10, 167 (1968).

11 R. Ligensa and W. Greiner, Nuclear Physics A92, 673 (1967).

12 R. L. Bramblett, J. T. Caldwell, R. R. Harvey, and S. C. Fultz, Phys. Rev. 133B, 869 (1964).

13 K. Okamoto, Progr. Theoret. Phys. Japan 15, 75 (1956).

14 M. A. Kelly, B. L. Berman, R. L. Bramblett, and S. C. Fultz, Phys. Rev. 179, 1194 (1969).

15 B. L. Berman, M. A. Kelly, R. L. Bramblett, J. T. Caldwell, H. S. Davis, and S. C. Fultz, Phys. Rev. 185, 1576 (1969b).

16 F. T. Kuchnir, P. Axel, L. Criegee, D. M. Drake, A. O. Hanson, and D. C. Sutton, Phys. Rev. 161, 1236 (1967).

17 L. M. Young, Thesis University of Illinois (1972 - unpublished).

18 W. Bertozzi, C. P. Sargent, and W. Turchinetz, Phys. Letters 6, 108 (1963).

19 M. Danos and W. Greiner, Phys. Rev. 138, B867 (1965).